



Published in final edited form as:

Nat Commun. 2012 ; 3: 1095. doi:10.1038/ncomms2094.

## ROBUST PHOTO-REGULATION OF GABA<sub>A</sub> RECEPTORS BY ALLOSTERIC MODULATION WITH A PROPOFOL ANALOG

Lan Yue<sup>1,2,\*</sup>, Michal Pawlowski<sup>3,\*</sup>, Shlomo S. Dellal<sup>4,\*</sup>, An Xie<sup>1,5</sup>, Feng Feng<sup>1</sup>, Thomas S. Otis<sup>4</sup>, Karol S. Bruzik<sup>3</sup>, Haohua Qian<sup>1,6</sup>, and David R. Pepperberg<sup>1,2,§</sup>

<sup>1</sup>Department of Ophthalmology and Visual Sciences, University of Illinois at Chicago, 1855 W. Taylor St., Chicago, IL 60612

<sup>2</sup>Department of Bioengineering, University of Illinois at Chicago, 851 S. Morgan St., Chicago, IL 60607

<sup>3</sup>Department of Medicinal Chemistry and Pharmacognosy, University of Illinois at Chicago, 833 S. Wood St., Chicago, IL 60612

<sup>4</sup>Department of Neurobiology, University of California at Los Angeles, 650 Charles E. Young Drive South, Los Angeles, CA 90095

<sup>5</sup>Department of Medicine, University of Illinois at Chicago, 840 S. Wood St., Chicago, IL 60612

<sup>6</sup>National Eye Institute, National Institutes of Health, 5635 Fishers Lane, Bethesda, MD 20892

### Abstract

Photochemical switches represent a powerful method for improving pharmacological therapies and controlling cellular physiology. Here we report the photo-regulation of GABA<sub>A</sub> receptors (GABA<sub>A</sub>Rs) by a derivative of propofol (2,6-diisopropylphenol), a GABA<sub>A</sub>R allosteric modulator, that we have modified to contain photo-isomerizable azobenzene. Using  $\alpha_1\beta_2\gamma_2$  GABA<sub>A</sub>Rs expressed in *Xenopus laevis* oocytes and native GABA<sub>A</sub>Rs of isolated retinal ganglion cells, we show that the *trans*-azobenzene isomer of the new compound (*trans*-MPC088), generated by visible light (wavelengths ~440 nm), potentiates the GABA-elicited response and at higher concentrations directly activates the receptors. *cis*-MPC088, generated from *trans*-MPC088 by UV light (~365 nm), produces little if any receptor potentiation/activation. In cerebellar slices, MPC088 co-applied with GABA affords bidirectional photo-modulation of Purkinje cell membrane current and spike-firing rate. The findings demonstrate photo-control of GABA<sub>A</sub>Rs by

Users may view, print, copy, and download text and data-mine the content in such documents, for the purposes of academic research, subject always to the full Conditions of use:[http://www.nature.com/authors/editorial\\_policies/license.html#terms](http://www.nature.com/authors/editorial_policies/license.html#terms)

<sup>§</sup>Corresponding Author: Dr. David R. Pepperberg, Department of Ophthalmology and Visual Sciences, University of Illinois at Chicago, 1855 W. Taylor St., Chicago, IL 60612, phone: 312-996-4262; [davipepp@uic.edu](mailto:davipepp@uic.edu).

<sup>\*</sup>These authors contributed equally to this work.

### AUTHOR CONTRIBUTIONS

K.S.B. and M.P. designed the chemical synthesis routes. M.P. performed the chemical syntheses and NMR experiments. The electrophysiological and spectrophotometric experiments were designed by L.Y., S.S.D., A.X., T.S.O., H.Q. and D.R.P., and performed by L.Y., S.S.D., A.X. and F.F. The manuscript was prepared by L.Y., D.R.P., S.S.D., T.S.O. and K.S.B., with all authors providing revisions.

The authors declare no competing financial interests.

an allosteric ligand and open new avenues for fundamental and clinically oriented research on GABA<sub>A</sub>Rs, a major class of neurotransmitter receptors in the central nervous system.

## INTRODUCTION

Synthetically modifying the neurotransmitter agonist of a postsynaptic receptor to contain a chemical photoswitch has been shown to afford photo-control of ionotropic receptors for acetylcholine and L-glutamate, through regulation of the access of the neurotransmitter moiety to its binding site<sup>1,2</sup>. A different approach is to engineer photo-regulation through a modulator rather than an agonist, by perturbing the receptor structure at a site distinct from the neurotransmitter binding pocket. The abundance and diversity of known allosteric modulators of receptor proteins suggest the feasibility of this alternative approach. Given that receptor modulators typically act in concert with endogenous signals in a neural network, a photo-switchable modulator could potentially enable relatively subtle conditional control of neuronal excitability.

GABA<sub>A</sub>Rs are pentameric ligand-gated ion channels that function as postsynaptic and extrasynaptic receptors for the inhibitory neurotransmitter  $\gamma$ -aminobutyric acid (GABA) in the brain and retina<sup>3-5</sup>. The  $\alpha_1\beta_2\gamma_2$  GABA<sub>A</sub>R, which consists of two  $\alpha_1$  subunits, two  $\beta_2$  subunits and a single  $\gamma_2$  subunit, is among the most abundant and widely distributed of this receptor type. A number of naturally occurring and synthetic low-molecular weight compounds are known to modulate the  $\alpha_1\beta_2\gamma_2$  GABA<sub>A</sub>R response to GABA<sup>3</sup>. Among the most extensively studied GABA<sub>A</sub>R modulators is propofol (Fig. 1a), a nonvolatile anesthetic that allosterically potentiates the GABA response and at high concentrations directly activates the receptor<sup>6-12</sup>. Behavioral studies indicate that propofol exerts its anesthetic actions by modulating GABA<sub>A</sub>Rs<sup>13,14</sup>. With the aim of developing photo-regulated  $\alpha_1\beta_2\gamma_2$  GABA<sub>A</sub>R-directed ligands, we have investigated propofol derivatives that contain azobenzene, a widely studied photoisomerizable chemical residue capable of bi-directional switching between *trans* and *cis* geometrical isomers<sup>1,2,15-20</sup>. Here we describe the development of a compound, termed MPC088 (Fig. 1a), that displays robust light-regulated activity at GABA<sub>A</sub>Rs. To our knowledge, the present study is the first to report photo-control of a neurotransmitter receptor by a *cis-trans* photoisomerizable compound derived from an allosteric ligand. The findings establish a new modality by which to regulate GABA<sub>A</sub>Rs, a receptor type of major importance to CNS function.

## RESULTS

### Light-regulated potentiation of $\alpha_1\beta_2\gamma_2$ GABA<sub>A</sub>R activity

Chemical synthesis and purification yielded MPC088 preparations consisting of the *trans*- and *cis*-isomers in proportions that were *trans*-dominant (typically, about 95%) (Supplementary Methods). Spectrophotometric and NMR data indicated that, as with unmodified azobenzene, UV light (wavelengths near 365 nm) isomerizes the *trans*-isomer MPC088 to the *cis* form that is stable for many hours in darkness, and visible (or blue) light (containing wavelengths near 440 nm) drives *cis* to *trans* isomerization (Supplementary Note 1 and Supplementary Figs. S1-S2).

In *Xenopus* oocytes expressing  $\alpha_1\beta_2\gamma_2$  GABA<sub>A</sub>Rs, 3  $\mu$ M GABA elicits a response ~4-10% of the saturation level, and was used to test for response enhancement by MPC088. When co-applied with 3  $\mu$ M GABA, MPC088 in predominantly the *trans*-isomer form increased the response in a concentration-dependent fashion (Fig. 1b) and exhibited a potency ~25 times that of propofol, as determined by the relationship of the MPC088 vs. propofol concentration for which the peak response amplitude was 50% of that elicited by 100  $\mu$ M GABA alone (Fig. 1c). By analogy with the known effects of propofol, this action of MPC088 could reflect contributions from both potentiation of the GABA response and direct receptor activation (i.e., direct agonist activity). We tested for potentiation by MPC088 at a concentration (1  $\mu$ M) associated with negligible direct activation, and specifically investigated the effect of light that isomerizes the azobenzene moiety (Figs. 1d-e). Co-applied 3  $\mu$ M GABA and 1  $\mu$ M *trans*-dominant MPC088 markedly potentiated the GABA response, and brief UV illumination presented during static bathing of the oocyte decreased the membrane current to a level near that elicited by GABA alone (Supplementary Note 2). This level of current was maintained in the ambient light after cessation of the UV illumination and, conversely, was increased by exposure to high-intensity visible light. The resumption of perfusion with co-applied GABA and *trans*-dominant MPC088 restored the membrane current to a level near that exhibited on initial presentation of the two compounds. By contrast, MPD021 (Fig. 1a) that lacks the propofol moiety showed no potentiation of the GABA response and failed to inhibit potentiation by MPC088 (Supplementary Note 3).

### Light-regulated direct activation of $\alpha_1\beta_2\gamma_2$ GABA<sub>A</sub>Rs

In addition to potentiation, *trans*-dominant MPC088 robustly activated  $\alpha_1\beta_2\gamma_2$  GABA<sub>A</sub>Rs (Fig. 2). The response elicited by *trans*-dominant MPC088 was graded with concentration, evident at concentrations as low as 4  $\mu$ M (Figs. 2a-b), and greater than the response to a matched concentration of *cis*-dominant MPC088. The maximum current generated by *trans*-dominant MPC088 was comparable with the peak current elicited by 100  $\mu$ M GABA, while that generated by propofol represented only about 40% of the 100  $\mu$ M GABA response. The potency of *trans*-dominant MPC088 exceeded that of propofol by ~25-fold, as determined by the concentrations of MPC088 vs. propofol required for a peak current equal to 40% of the 100  $\mu$ M GABA-alone response (Fig. 2b). The MPC088-elicited response was eliminated by the GABA<sub>A</sub>R channel blocker picrotoxin (PTX)<sup>21</sup>, but was not sensitive to gabazine (SR-95531) – a competitive GABA antagonist<sup>22,23</sup> – and was only partially antagonized by bicuculline<sup>8,24</sup> (Fig. 2b inset). These properties, which are shared by the known GABA<sub>A</sub>R allosteric activators alphaxalone<sup>10,22</sup> and pentobarbital<sup>24,25</sup>, suggested that MPC088 activates the receptors by binding at a site distinct from the GABA-binding site. UV illumination presented during static bathing reduced the MPC088-elicited current, and visible light reversed the effect of UV exposure (Figs. 2c-d). Furthermore, repeated pulses of UV light presented on a background of continuous visible light during MPC088 treatment yielded cyclic changes in response amplitude (Fig. 2e). Together, the data of Figures 1-2 do not rule out an action of *cis*-MPC088 in receptor potentiation or direct activation (Supplementary Note 4), but indicate that any such activity is much weaker than that of the *trans*-isomer.

### Activity at GABA<sub>A</sub>Rs of differing subunit composition

Propofol is known to modulate GABA<sub>A</sub> receptors that contain a  $\beta$  subunit. To determine whether *trans*-MPC088 is active at other  $\beta$ -containing GABA<sub>A</sub> subtypes, we tested the compound in oocytes-expressing  $\alpha_1\beta_3\gamma_2$ , a GABA<sub>A</sub>R that like  $\alpha_1\beta_2\gamma_2$ , is widely expressed in CNS neurons<sup>3,26-28</sup>; and at  $\alpha_4\beta_3\delta$ , a subtype that is typically expressed extrasynaptically and exhibits high sensitivity to GABA<sup>3,5,29</sup>. *Trans*-dominant MPC088 showed potentiating activity on both receptor types (Fig. 3a), and this activity was reduced by UV illumination (not shown). With co-applied 3  $\mu$ M GABA (representing  $\sim$ EC<sub>8</sub>), the  $\alpha_1\beta_3\gamma_2$  GABA<sub>A</sub>R response function obtained with *trans*-dominant MPC088 closely resembled that determined for the  $\alpha_1\beta_2\gamma_2$  subtype. By contrast, the *trans*-MPC088 response function obtained for  $\alpha_4\beta_3\delta$  with co-applied 50 nM GABA ( $\sim$ EC<sub>8</sub>) approached a plateau representing  $\sim$ 42% of the response amplitude obtained with high GABA concentration. The low plateau level of the  $\alpha_4\beta_3\delta$  response to *trans*-MPC088 did not reflect a general insensitivity to propofol-based compounds, since co-applied 200  $\mu$ M propofol and 50 nM GABA yielded a response representing  $1.2 \pm 0.1$ -fold ( $n = 4$ ) that of the saturating GABA-alone response. In addition, the direct agonist activity of *trans*-MPC088 at  $\alpha_4\beta_3\delta$  was much lower than those at  $\alpha_1\beta_3\gamma_2$  and  $\alpha_1\beta_2\gamma_2$  (Fig. 3b). Thus, *trans*-MPC088, like propofol, modulates multiple types of  $\beta$ -containing GABA<sub>A</sub> receptors, albeit with different efficacy. We also tested the activity of *trans*-dominant MPC088 at receptors containing the  $\beta$ -subunit substitution N265M, a mutation that markedly reduces the action of propofol both *in vitro* and *in vivo*<sup>13,30</sup>. These experiments specifically involved comparison of the normalized responses of  $\alpha_1\beta_3\gamma_2$  and  $\alpha_1\beta_3$ (N265M) $\gamma_2$  GABA<sub>A</sub>Rs to *trans*-MPC088 (1  $\mu$ M) and co-applied GABA. Response enhancement by *trans*-MPC088 was substantial at both receptor types, but that for  $\alpha_1\beta_3$ (N265M) $\gamma_2$  ( $2.9 \pm 0.8$ -fold,  $n=4$ ) was significantly smaller than that for the wildtype  $\alpha_1\beta_3\gamma_2$  ( $4.4 \pm 1.3$ -fold,  $n=5$ ;  $p=0.03$ , two-sample *t*-test) (Supplementary Fig. S3). Like propofol, *trans*-MPC088 lacked both potentiating and direct agonist activity on oocytes expressing the GABA<sub>A</sub>R subtype that consists of a pentameric assembly of  $\rho 1$  subunits<sup>31</sup>.

### Receptor-tethered MPC088 analog

MPC088 is a freely diffusible compound and can be removed by superfusion of the oocyte with Ringer. We asked whether covalent tethering of a similar compound to a suitably modified receptor produces persistent potentiation and/or activation. MPC100 (Fig. 1a), prepared by coupling a maleimide-terminated 24-mer poly(ethylene glycol) (PEG) linker to the free amino group of MPC088, was tested on oocytes expressing a cysteine substitution at position 79 of the single  $\gamma$  subunit of  $\alpha_1\beta_2\gamma_2$  [ $\alpha_1\beta_2\gamma_2$ (A79C)]<sup>32,33</sup>, abbreviated as  $\gamma$ -79C. The thiol group of the cysteine residue allowed covalent anchoring of MPC100<sup>15,17,19</sup>. Oocytes expressing  $\gamma$ -79C GABA<sub>A</sub>Rs, following incubation with *trans*-dominant MPC100 and then superfusion with unsupplemented Ringer to remove untethered compound, exhibited persistent potentiation of the GABA response (Figs. 4a-b), which was sensitive to UV and visible light (Fig. 4c). These effects of illumination resembled those displayed by wildtype  $\alpha_1\beta_2\gamma_2$  GABA<sub>A</sub>R-expressing oocytes in the presence of co-applied GABA and MPC088 (compare Figs. 1d and 4c), although the extent of UV-induced de-potentiation observed with the tethered MPC100 was less than that determined on similar treatment with (diffusible) MPC088. The smaller excursion of de-potentiation likely resulted from the inability of the

UV stimulating light, which was delivered from above the (opaque) oocyte, to efficiently access MPC100 tethered to the lower, approximately hemispherical surface of the cell.

Treatment of  $\gamma$ -79C-expressing oocytes with *trans*-dominant MPC100 led to a greater (i.e., more negative) baseline current, and UV illumination produced an opposite change (Fig. 4c; note the relationship of the dotted reference lines i and ii). To test whether the baseline change reflected continuing, direct activation by the tethered MPC100 in the absence of GABA, we investigated the effect of PTX presented before and after MPC100 treatment. PTX application to MPC100-treated and then washed cells reversibly reduced the baseline current by  $85 \pm 7\%$  ( $n = 5$ ) (Fig. 4d, traces i-ii). UV (i.e., *cis*-generating) illumination delivered during PTX treatment did not further reduce the baseline amplitude, but inhibited baseline recovery following PTX removal, consistent with a UV-induced reduction in the amount of *trans*-MPC100 present (Fig. 4d, trace iii). Furthermore, UV and visible light delivered to MPC100-treated  $\gamma$ -79C-expressing oocytes produced, respectively, decreases and increases in membrane current qualitatively similar to those exhibited by wildtype  $\alpha_1\beta_2\gamma_2$  GABA<sub>A</sub>Rs in the presence of *trans*-MPC088 alone (Figs. 4e-f). Thus, the larger baseline current persisting after MPC100 treatment (Fig. 4c) reflected sustained, direct activation of the receptor by tethered *trans*-MPC100.

These persistent effects of MPC100 required the  $\gamma$ -79C modification. While MPC100 exhibited potentiation on wildtype  $\alpha_1\beta_2\gamma_2$  GABA<sub>A</sub>Rs (albeit to an extent less than that exhibited by MPC088), this effect was eliminated by Ringer perfusion (Supplementary Note 5 and Supplementary Fig. S4). In addition, on  $\gamma$ -79C-expressing oocytes, pre-treatment with the thiol-reactive compound methyl-(PEG)<sub>11</sub>-maleimide blocked the activity of subsequently applied MPC100 (Supplementary Note 6). These findings indicate a dependence of MPC100's persistent activity on tethering specifically at the engineered cysteine site of the  $\gamma$ -79C receptor.

### Activity at GABA<sub>A</sub>Rs of retinal ganglion cells

To test whether native neuronal GABA<sub>A</sub>Rs respond to MPC088, we examined retinal ganglion cells (RGCs), a cell type known to abundantly express GABA<sub>A</sub>Rs<sup>34-37</sup>. When presented to single dissociated RGCs of rat retina, 10  $\mu$ M *trans*-dominant MPC088 produced, on average, an approximately 5-fold potentiation of the response elicited by 2  $\mu$ M GABA, while *cis*-dominant MPC088 exhibited much less potentiation activity (Fig. 5a). At 30  $\mu$ M, *trans*-dominant MPC088 alone produced a membrane current response whose peak amplitude amounted, on average, to 5% of the cell's response to 200  $\mu$ M GABA (Fig. 5b, inset). However, at 60  $\mu$ M, the agonist effect increased to  $43 \pm 9\%$  of the response to 200  $\mu$ M GABA ( $n = 7$ ), and pre-treatment of *trans*-dominant MPC088 with UV light reduced this agonist activity by  $88 \pm 6\%$  ( $n = 4$ ;  $p = 0.002$ , two-sample *t*-test) (Fig. 5b). Co-application of 100  $\mu$ M PTX virtually eliminated the ganglion cell response to 2  $\mu$ M GABA + 10  $\mu$ M *trans*-dominant MPC088, and to 60  $\mu$ M *trans*-dominant MPC088 alone (Supplementary Note 7 and Supplementary Fig. S5), consistent with mediation of *trans*-MPC088's potentiation and direct activation by GABA<sub>A</sub>Rs.

## Photo-regulation of GABA<sub>A</sub>Rs of cerebellar Purkinje neurons

To evaluate the efficacy of MPC088 in GABA<sub>A</sub>R-expressing cells *in situ*, we conducted whole-cell voltage-clamp experiments on Purkinje neurons (PNs) in parasagittal slices from mouse cerebellum<sup>38,39</sup> (Fig. 6 and Supplementary Methods). PNs are known to express GABA<sub>A</sub>Rs of the  $\alpha_1\beta_2/3\gamma_2$  forms<sup>26-28</sup>. Figure 6a shows the experimental setup, indicating how blue and UV light sources were combined in the epifluorescence pathway of an upright microscope. Currents were evoked in the PNs by applying 10  $\mu$ M GABA from a local pressure pipette that also contained 30  $\mu$ M *trans*-dominant MPC088. UV illumination during the elicited response markedly decreased the membrane current; conversely, blue light enhanced the current (Fig. 6b). To determine whether these effects of light required the presence of MPC088, we performed similar experiments on the same cell by replacing the pressure pipette with one that contained only GABA (Fig. 6c) or GABA plus propofol (Fig. 6d). By contrast with the Figure 6b results, there was little or no light-induced current change under either condition. To quantify these results, we measured the current change in response to transitions from UV to blue light and from blue to UV light (Fig. 6e). We found that the current changes produced by these transitions were opposite and, on average, equal in magnitude (mean ratio of absolute current magnitude in response to blue $\rightarrow$ UV / UV $\rightarrow$ blue was  $1.00 \pm 0.01$ , a value that did not differ significantly from unity;  $p = 0.86$ ; one-sample t-test,  $n = 7$ ) (Fig. 6f). Together, these results demonstrate that MPC088 directly modulates GABA<sub>A</sub>Rs of cerebellar PNs *in situ*.

We also examined the effects of MPC088 on action potential firing in PNs of the cerebellar slice. These experiments were similar to those described above, except that the cells were recorded under current-clamp in order to allow the cell to spike. To each of the PNs described in Figures 7a-b, we first delivered GABA (10  $\mu$ M) plus *trans*-dominant MPC088 (30  $\mu$ M) by pressure application, and then exposed the cell to sequences of UV-Blue-UV light. Exposure to GABA + *trans*-dominant MPC088 decreased the firing rate by approximately 50%, on average (Fig. 7b). Furthermore, in all of the 8 investigated cells, the UV-Blue-UV flash sequence led, respectively, to an increase, decrease and increase in firing rate. Overall, the firing rate produced by blue light was  $52 \pm 14\%$  of that produced by UV light. In 3 of the 8 PNs, blue light decreased the firing rate to  $<20\%$  of that exhibited during the UV illumination, and one PN exhibited a blue-light-induced complete cessation of spiking that was reversed by subsequent UV. As a negative control, we exposed cells to the UV-Blue-UV light sequence but in the absence of GABA/MPC088 application. In these cells, there was no significant change in firing rate with any of the light flashes (Fig. 7c). Together, these data indicate a reversible, light-dependent action of MPC088 on PN spike-firing rate.

To test for direct agonist activity of MPC088 on PNs, we perfused cerebellar slices with recirculating 30  $\mu$ M MPC088 (the maximal MPC088 concentration we could reliably maintain solubilized in bicarbonate-buffered solution). MPC088 was converted to *cis*-dominant form by a 2-min exposure to UV light (LED, 365 nm/160 mW, Mouser, Inc., Mansfield, TX; LED driver, 700 mA BuckPuck DC Driver, Quadica Developments, Inc., Brantford, Ontario, Canada), before its dilution into the recirculating external solution. The same LED was then used to continuously UV-illuminate the recirculating solution for the

duration of the experiment. We then obtained whole-cell voltage clamp recordings from PNs and determined the change in membrane current produced by alternating blue and UV illumination of the slice, as in the Figure 6 experiments. Of 44 cells examined, only 28 exhibited a current change  $>18$  pA, which is the average amplitude of the Blue-to-UV light currents from the vehicle and propofol conditions described in Figure 6. The average response from this subset of 28 cells was  $80 \pm 13$  pA. We then sought to test whether these currents were due to an agonist action of the drug, as opposed to a modulatory action occurring in concert with low levels of endogenous GABA present in the slice<sup>40</sup>. To discern modulation, we analyzed the effect of added  $30 \mu\text{M}$  gabazine<sup>22,23</sup>, a condition expected to inhibit the potentiating action of MPC088 (i.e., to inhibit response enhancement dependent on endogenous GABA) but not to affect the direct agonist activity of MPC088 (Fig. 2). In all but one of eight cells that exhibited light-evoked responses of  $>50$  pA to the Blue-to-UV switch, gabazine ( $30 \mu\text{M}$ ) reduced the current to below the vehicle level of 18 pA (Fig. 8a-b). The average current remaining after gabazine treatment represented  $11 \pm 3$  % of the pre-gabazine current (Fig. 8b). Even for the cell exhibiting the highest response of the 44 cells tested, gabazine completely abolished the response (Fig. 8a). Thus, at concentrations comparable to or lower than  $30 \mu\text{M}$ , *trans*-MPC088 in cerebellar tissue is modulatory (endogenous GABA-dependent) rather than agonistic.

### Specificity of MPC088 for GABA<sub>A</sub>Rs on neurons

To further address whether MPC088 has non-specific effects on excitability, we analyzed the spikes elicited in the experiment described in Figure 7. We examined spikes recorded during exposure to GABA/MPC088 (“puff”) and under conditions in which MPC088 was absent but in which the Purkinje cell received the UV/Blue/UV light sequence (“no-puff”). Three action potential (AP) parameters were measured: peak amplitude, half width, and maximum rise slope. Parameters were obtained from spikes occurring in the same 1-s epochs in which average firing rate was significantly modulated by MPC088 (see Fig. 7b-c). AP waveform parameters were calculated for pre-puff, blue light, and UV epochs. Average values in the pre-treatment epochs for puff and no-puff did not significantly differ (Spike Amplitude (mV),  $52 \pm 2$  and  $51 \pm 2$ ; Half Width (ms),  $0.61 \pm 0.03$  and  $0.57 \pm 0.03$ ; Maximum Rise Slope (mV/ms),  $150 \pm 10$  and  $161 \pm 13$ ;  $p > 0.4$ , unpaired t-test). In addition, for each parameter, we normalized the average values for each cell and for each epoch, to the averages in the pre-treatment epochs (pre-puff, pre-light). This analysis of excitability showed first, that the only measureable effects on AP waveform are MPC088-independent and caused by light exposure, and second, that the effect size of light is extremely small (less than 2%; Supplementary Fig. S6 and Supplementary Note 8).

To test whether MPC088 affects excitatory synaptic transmission, we carried out whole-cell voltage-clamp recordings in CA1 pyramidal neurons of mouse hippocampus. As in the experiments of Figure 8, these recordings were obtained with perfusion of the slice with *cis*-dominant MPC088 ( $30 \mu\text{M}$ ) under recirculation. PTX ( $100 \mu\text{M}$ ) was also included in the external solution to block GABA<sub>A</sub>Rs. We evoked EPSCs by stimulating the Schaffer collaterals with a bipolar matrix microelectrode (FHC, Inc., Bowdoin, ME), and recorded at a holding potential of +40 mV to uncover the NMDA receptor (NMDAR) component of the EPSC. We also presented paired electrical stimuli separated by 80 ms to assess possible

effects of MPC088 on short-term plasticity. Each cell was given 20 interleaved trials in which the cell was exposed to two 0.1-s UV pulses surrounding a 1-s period of either blue light or no light (Supplementary Fig. S7 and Supplementary Methods). The effectiveness of the 0.1-s UV and the 1-s blue stimuli in photoconverting MPC088 was confirmed in separate experiments using 30  $\mu$ M MPC088 and 3  $\mu$ M GABA on the same preparation. To quantify the effects of MPC088 on AMPA receptors (AMPA) and NMDARs, we measured, for the first EPSC of the pair, the peak current and the current just prior to the second stimulus, which reflect AMPAR and NMDAR components, respectively, of the EPSC<sup>41</sup>. Neither AMPAR-mediated nor NMDAR-mediated components of the EPSC were significantly altered by blue light (Supplementary Fig. S7b). Additionally, blue light had no significant effect on the decay of the compound current (average  $\tau$  from single-exponential fitting to the decay of the second EPSC: Blue off,  $131 \pm 11$  ms; Blue on,  $131 \pm 11$  ms;  $p=0.89$ , paired t-test). There was also no significant effect of blue light on the paired-pulse ratio (PPR, measured as Peak(2nd EPSC)/Peak(1st EPSC): Blue off,  $1.72 \pm 0.07$ ; Blue on,  $1.85 \pm 0.14$ ;  $p=0.34$ , paired t-test). Together, these results indicate that MPC088 does not significantly affect presynaptic function and that it has negligible actions on AMPAR-mediated and NMDAR-mediated EPSCs.

## DISCUSSION

The results demonstrate that MPC088, a photoisomerizable compound derived from the allosteric ligand propofol, exerts a highly potent and light-sensitive regulation of GABA<sub>A</sub> receptors. Light of differing wavelength can reversibly and in a quasi-stable manner interconvert the relatively active and inactive isomers of MPC088; this distinguishes the compound from a photosensitive ligand in which light activates the ligand by excitation of a fluorescent moiety<sup>42</sup> or by irreversibly eliminating a protective (caging) structural component. In addition to conferring pronounced light-sensitivity to the receptor, MPC088 in its active (*trans*) form exhibits a potency considerably exceeding that of propofol itself. Our data indicate that the propofol moiety is required for activity, but it remains to be determined whether the high potency of MPC088 is due in addition to specific receptor-binding interactions with the butyryl, azobenzene and/or ethylenediamine moieties of the compound. Such a possibility is consistent with the finding that the  $\alpha_1\beta_3(\text{N265M})\gamma_2$  GABA<sub>A</sub>R, which contains a substitution that strongly decreases the *in vivo* action of propofol<sup>13</sup>, exhibits reduced but still substantial sensitivity to *trans*-MPC088. Furthermore, while the present results argue against a direct agonist action of *trans*-MPC088 on ligand-gated ion channels of cerebellar PNs other than GABA<sub>A</sub>Rs, the broad possibility remains that *trans*-MPC088 has physiological effects on non-GABA<sub>A</sub>R ion channels or other surface proteins of neural tissue. Particularly at higher concentrations, some broader activity of the compound would likely be tolerable, as propofol itself, while most active at GABA<sub>A</sub>Rs<sup>14</sup>, is known to have effects on other cellular targets<sup>43</sup>.

We have also examined the properties of MPC100, a tetherable derivative of MPC088 that, via its terminating maleimide group, covalently binds to the cysteine-substituted  $\gamma$ -79C mutant form of the  $\alpha_1\beta_2\gamma_2$  GABA<sub>A</sub>R. The tethered compound exhibits persistent, light-regulated potentiating and activating effects on GABA<sub>A</sub>Rs. Thus, the tetherable MPC100 may have application in approaches that involve neuronal expression of a genetically



engineered  $\alpha_1\beta_2\gamma_2$  GABA<sub>A</sub>R to which the photoswitch could be anchored, as in previous studies of potassium channels and L-glutamate receptors<sup>15,17,19</sup>. Furthermore, by contrast with previous structures designed for photo-control of transmembrane ion channels<sup>1,15,17,19</sup>, a relatively long linear chain (PEG<sub>24</sub>) separates the regulating structure (MPC088 moiety) from the tethering moiety (maleimide). Beyond demonstrating that a long and flexible hydrophilic linker (and resultant high conformational entropy) can preserve substantial physiological activity of the distal MPC088 moiety, properties exhibited by MPC100 suggest the potential workability of other remote locations on the GABA<sub>A</sub>R itself for modulator attachment, or conjugation of the modulator to an affinity reagent designed for binding to the extracellular domain of the native GABA<sub>A</sub>R. As a general route to controlling neuronal activity with a modulating ligand, covalent binding of an introduced reactive (e.g., maleimide-terminated) ligand to an engineered receptor site offers the advantage, in principle, of defining the precise receptor subtype<sup>4</sup> on which the ligand will act. However this approach presents possible challenges relating to the need for inducing expression of the engineered receptor in the target cell type, and for avoiding problematic binding of the reactive ligand to unintended sites (e.g., other cysteine-containing surface proteins) on both the target cells and others.

The wide distribution of  $\alpha_1\beta_2\gamma_2$  GABA<sub>A</sub>Rs in central nervous system (CNS) tissues and the clinical importance of propofol encourage the investigation of MPC088 as a pharmacological tool in studies of CNS neural circuits. Toward this end we have demonstrated that the compound reversibly modulates GABA currents in retinal neurons and cerebellar PNs and that it can be used to reversibly control spiking output of PNs. Given that PNs are intrinsically active at constant rates<sup>38,39</sup>, they are useful for examining this modulation because their spike rate gives a continuous readout of excitability.

In providing the ability to control circuit excitability with spatial and temporal precision, switchable modulators of neural activity open new possibilities for exploring the links between neuronal activity and behavior. For example, MPC088 and related diffusible compounds could allow regional induction of anesthesia through the use of implanted optical fibers or a head-fixed preparation. This approach could be used to explore which brain regions are most important for anesthesia and sedation. Clinical contexts in which a photo-switchable GABA<sub>A</sub>R modulator might be useful include diseases of hyperexcitability, such as epilepsy<sup>44-47</sup>. Propofol is known to be an effective therapeutic for intractable epilepsy, although side effects are a concern<sup>48-50</sup>. Photo-switchable propofol analogs, in combination with localized optical stimulation<sup>51</sup> and appropriate electrical monitoring, might enable a reduction of side effects in treating epilepsies, by employing spatially precise, optically-regulated receptor modulation specifically during bouts of hyperexcitability. Furthermore, even with a diffusible modulator, focally directed illumination could allow spatially restricted actions of the anti-epileptic drug around seizure foci.

The photosensitivity and potency of MPC088 raise the possibility that compounds of this type might be used therapeutically in visual disorders. GABA<sub>A</sub>Rs are known to mediate visual signaling at multiple sites within the retina<sup>34,35,37,52-54</sup>; GABA<sub>A</sub>Rs of retinal bipolar and ganglion cells are sensitive to propofol<sup>55,56</sup>; and, as in oocyte-expressed  $\alpha_1\beta_2\gamma_2$

GABA<sub>A</sub>Rs, responses of retinal ganglion cells are potentiated and directly activated specifically by the *trans*-isomer of MPC088 (Fig. 5). In diseases involving degeneration of the retina's rod and cone photoreceptors, MPC088-inspired constructs of optimized wavelength sensitivity and relaxation kinetics<sup>57</sup>, and containing an affinity reagent-based anchor to provide cell-targeting specificity, may have application as a vision restoration therapy, by establishing a photosensitivity of inner retinal neurons that effectively bypasses the dysfunctional rods and cones.

## METHODS

### Electrophysiological recordings

Electrophysiological experiments were conducted on *Xenopus laevis* oocytes expressing  $\alpha_1\beta_2\gamma_2$  GABA<sub>A</sub>Rs (rat  $\alpha_1$ , rat  $\beta_2$  and human  $\gamma_2S$ ); on single, isolated ganglion cells of rat retina; on Purkinje neurons (PNs) in acute slice preparations of mouse cerebellum; and on CA1 neurons in acute slice preparations of mouse hippocampus. Animal care and all procedures involving the use of animals were conducted in accordance with institutional policies of the University of Illinois at Chicago (for *Xenopus laevis* and rats), and with the approval of the Chancellor's Animal Research Committee (Institutional Animal Care and Use Committee) at the University of California, Los Angeles (for mice).

### *Xenopus laevis* oocytes

Oocytes expressing  $\alpha_1\beta_2\gamma_2$  receptors (rat  $\alpha_1$ , rat  $\beta_2$  and human  $\gamma_2S$ ) were prepared and studied by two-electrode voltage-clamp recording<sup>58</sup> (holding potential: -70 mV; amplifier: GeneClamp500B; Axon Instruments, Foster City, CA). Unless otherwise indicated, oocytes were superfused with Ringer solution (physiological saline) at a rate of ~1 mL/min. The experiments of Figures 1d-e, 2c-e and S4 involved periods of static bathing, i.e., halted superfusion. The  $\gamma_2(A79C)$  subunit was prepared by site-directed mutagenesis. Oocyte electrophysiological experiments were carried out in room light. A UV light-emitting diode (peak wavelength: 365 nm; Hamamatsu Photonics, Japan) and a microscope illuminator (white light; Schott Fostec, Auburn, NY) provided UV and visible stimulating light. As measured at the position of the oocyte, the intensity of the UV light at 365 nm was 220  $\mu\text{W}/\text{mm}^2$ . At 440 nm, the nominal strength of the visible (white) light (referred to as high-intensity visible light) was 28  $\mu\text{W}/\text{mm}^2$ , and that of the ambient room illumination was 0.045  $\mu\text{W}/\text{mm}^2$ . In all experiments, low-intensity visible light from the microscope illuminator (3  $\mu\text{W}/\text{mm}^2$  at 440 nm) was present at all times except those involving high-intensity visible illumination. Electrophysiological data were obtained using Clampex 8.2 (Axon Instruments), analyzed using Clampfit 10.0 (Axon Instruments) and OriginPro7.5 (OriginLab, Northampton, MA).

### Retinal ganglion cells of rat

Experiments were conducted on enzymatically dissociated ganglion cells obtained from adult Sprague-Dawley rats (male and female, 6-16 weeks of age) (Charles River Laboratories, Wilmington, MA). Procedures for euthanasia, isolation of the retina, and the dissociation of retinal cells were as described previously<sup>59</sup> except that the period of retinal cell dissociation was shortened from 40 min to 20 min. Isolated ganglion cells were

identified on the basis of their morphological appearance and the presence of a large voltage-gated sodium current. Whole-cell patch-clamp techniques similar to those described<sup>59</sup> were used to record membrane current responses to test agents. The patch pipette with a resistance of 8-12 M $\Omega$  was pulled in two stages using a micro-electrode puller (Model PP830, Narishige Group, Tokyo, Japan). The pipette was filled with an intracellular solution containing 95 mM CsCH<sub>3</sub>SO<sub>3</sub>, 20 mM TEA-Cl, 10 mM glutamic acid, 1 mM BAPTA, 10 mM HEPES, 8 mM phosphocreatine di(tris), 1 mM MgATP and 0.2 mM Na<sub>2</sub>GTP; pH adjusted to 7.2 with CsOH. Cells were clamped at 0 mV (Axopatch 200B amplifier; Axon Instruments), and experimental runs were controlled by pCLAMP system software (Axon Instruments). Electrophysiological data were obtained in response to test compounds dissolved in physiological saline (Ringer solution) that consisted of 135 mM NaCl, 5 mM KCl, 2 mM CaCl<sub>2</sub>, 2 mM MgCl<sub>2</sub>, 10 mM glucose, and 5 mM HEPES, pH 7.4. Supplementation of aqueous test solutions with MPC088 was carried out by adding an aliquot of a stock solution containing the compound dissolved in dimethyl sulfoxide (DMSO). In all experiments, the amount of carrier DMSO present in the applied test solution was <1% (v/v). Test solutions were delivered from separate reservoirs by a multi-channel perfusion system. The same UV-LED used in the oocyte experiments was used for UV illumination of MPC088-supplemented test solutions. For preparation of *cis*-dominant MPC088, the test solution of initially *trans*-dominant compound underwent a 5-min UV illumination prior to its placement in the perfusion reservoir. All preparative procedures were performed in the dark, and the reservoirs and perfusion lines were light-protected with aluminum foil. As in the oocyte experiments, data were analyzed with Clampfit and plotted with Origin. Unless otherwise stated, numerical data from replicate experiments are presented as mean  $\pm$  SD, and all statistical analyses of data obtained from oocytes and from retinal ganglion cells employed a two-sample *t*-test.

### Cerebellar Purkinje neurons from mice

Experiments on cerebellar PNs employed acute slices obtained from cerebella of 16-30 day-old C57/BL6 mice (Charles River Laboratories). After induction of deep anesthesia with isoflurane, mice were decapitated, and the cerebellum vermis was removed and placed in an ice-cold cutting solution containing (in mM): 85 NaCl, 2.5 KCl, 0.5 CaCl<sub>2</sub>, 4 MgCl<sub>2</sub>, 1.25 NaH<sub>2</sub>PO<sub>4</sub>, 24 NaHCO<sub>3</sub>, 25 glucose, and 75 sucrose. A Leica VT1000 vibratome was used to cut 250  $\mu$ m thick, sagittal slices from the cerebellar vermis. Slices were then placed in an external recording solution containing (in mM): 119 NaCl, 2.5 KCl, 2 CaCl<sub>2</sub>, 1 MgCl<sub>2</sub>, 1 NaH<sub>2</sub>PO<sub>4</sub>, 26.2 NaHCO<sub>3</sub>, and 25 glucose. The solution was warmed to 35°C for 15-20 min and then allowed to reach room temperature. Both the cutting solution and the recording solution were continuously bubbled with 95% O<sub>2</sub> / 5% CO<sub>2</sub>, and the recording solution was perfused at the rate of 2-4 mL/min.

Whole-cell voltage-clamp recordings were carried out at room temperature from PNs with an Axopatch 200A amplifier (Axon Instruments), and the neurons were held at -70 mV. Recording pipettes had bath resistances of 2-6 M $\Omega$  and were pulled using a horizontal micropipette puller (Model P-1000 Flaming/Brown Micropipette Puller, Sutter Instrument Company, Novato, CA). The internal solution for voltage clamp (Figs. 6 and 8) contained (in mM): 140 CsCl, 3 NaCl, 10 HEPES, 2 MgCl<sub>2</sub>, 4 ATP, 0.4 GTP, 1 EGTA, 10 TEA-Cl

and 5 QX-314 Br (to block respectively,  $K_v$  and  $Na_v$  channels), and pH was adjusted to 7.4 with CsOH. Cs-based internal solutions prevented a small, UV light-elicited, transient outward current that was seen in the absence of GABA or MPC088. In some recordings  $CdCl_2$  (100  $\mu$ M) was included in the external solution to block synaptic transmission. Although we found no differences in the magnitudes of the MPC088-dependent currents, this had two benefits; it reduced spontaneous synaptic activity which would otherwise appear as high frequency noise on the traces, and it confirmed that MPC088 actions were cell-autonomous.

Whole-cell current-clamp recordings from PNs were carried out at room temperature with the same equipment as described above. Recording pipettes had bath resistances of 6-9 M $\Omega$ . The internal solution substituted 126-130 mM  $KMeSO_3$  for CsCl/(TEA-Cl) and contained 5 mM EGTA. In some cases internal solutions for current clamp included 5 mM phosphocreatine and KCl substituted for NaCl to yield a final chloride concentration of 14 mM. Where appropriate, distilled water was added to adjust final osmolarity. In some cases positive current was injected into the PNs to elicit spiking. Local drug application to the PNs was achieved with a glass pipette (2-3  $\mu$ m tip diameter) filled with the solution containing the indicated compounds dissolved in filtered external recording solution. Pressure pulses (0.5 to 2 psi) were provided by a Picospritzer II (Parker Hannifin Co., Cleveland, OH). Data from cells were excluded from analysis if there was no detectable decrease in firing rate with GABA + MPC088 application. They were also excluded if the average baseline (2-s epoch before drug application) firing rates fell outside the range 5 to 100 Hz, or if the cell stopped firing completely in the midst of the trial and did not recover by the end of the trial.

Pulses of UV light were presented to the tissue by shuttering a 100 W mercury arc lamp. Light from this source was collimated and focused through the objective lens of the recording apparatus. The broad-spectrum light from the arc lamp passed through an excitation filter (366 nm; full-width at half-maximum, 16.6 nm; Semrock, Inc., Rochester, NY) to isolate the UV component, and reflected off a dichroic mirror (409 nm cutoff, Semrock, Inc.) (Fig. 6a). The blue light source was a 470 nm LED (Quadica Developments, Inc., Brantford, Ontario, Canada) that was connected to a beamsplitter cube (Siskiyou Designs, Grants Pass, OR) located in the infinity space above the objective. The blue light was reflected by the dichroic mirror (500 nm cutoff, Chroma Technology Co., Bellows Falls, VT) positioned in the beamsplitter cube such that it passed through the 409 nm dichroic mirror in the UV filter cube to reach the slice. This configuration allowed UV and blue light to be combined in the epifluorescence path and independently controlled. To minimize exposure of the slice preparation and MPC088-containing solutions to ambient room light, the experimental apparatus housing the cerebellar slice, microscope, micro-manipulators and perfusion lines was shielded by a dark curtain, and a photographic safe-light was used inside the area housing these components. Illumination from the microscope lamp used for visual inspection of the tissue passed through a Wratten 2 29 filter that attenuated wavelengths below 600 nm. All data from experiments on PNs are presented as mean  $\pm$  SEM.

## Supplementary Material

Refer to Web version on PubMed Central for supplementary material.

## Acknowledgments

We thank Drs. Robert F. Standaert, Hélène A. Gussin and Deborah M. Little for helpful discussions, Dr. Martin Wallner for providing cDNA for the  $\alpha_4$ ,  $\beta_3$ ,  $\beta_3(N265M)$  and  $\delta$  GABA<sub>A</sub>R subunits, and Dr. Matthew Shtrahman, Ms. Vivy Tran, Ms. Tara Nguyen and Dr. Joyce Wondolowski for technical assistance. Supported by NIH grants EY016094, EY001792 and AA01973; the Daniel F. and Ada L. Rice Foundation (Skokie, IL); Hope for Vision (Washington, DC); the Beckman Initiative for Macular Research (Los Angeles, CA); the American Health Assistance Foundation (Clarksburg, MD); Research to Prevent Blindness (New York, NY); and by award UL1RR029879 from the University of Illinois at Chicago Center for Clinical and Translational Science (CCTS).

## References

1. Lester HA, Krouse ME, Nass MM, Wassermann NH, Erlanger BF. A covalently bound photoisomerizable agonist: comparison with reversibly bound agonists at *Electrophorus* electroplaques. *J Gen Physiol.* 1980; 75:207–232. [PubMed: 6246192]
2. Volgraf M, et al. Reversibly caged glutamate: a photochromic agonist of ionotropic glutamate receptors. *J Amer Chem Soc.* 2007; 129:260–261. [PubMed: 17212390]
3. Farrant M, Nusser Z. Variations on an inhibitory theme: phasic and tonic activation of GABA<sub>A</sub> receptors. *Nature Rev Neurosci.* 2005; 6:215–229. [PubMed: 15738957]
4. Olsen RW, Sieghart W. GABA<sub>A</sub> receptors: subtypes provide diversity of function and pharmacology. *Neuropharmacology.* 2009; 56:141–148. [PubMed: 18760291]
5. Mortensen M, Ebert B, Wafford K, Smart TG. Distinct activities of GABA agonists at synaptic- and extrasynaptic-type GABA<sub>A</sub> receptors. *J Physiol.* 2010; 588:1251–1268. [PubMed: 20176630]
6. Hales TG, Lambert JJ. The actions of propofol on inhibitory amino acid receptors of bovine adrenomedullary chromaffin cells and rodent central neurones. *Br J Pharmacol.* 1991; 104:619–628. [PubMed: 1665745]
7. Orser BA, Wang LY, Pennefather PS, MacDonald JF. Propofol modulates activation and desensitization of GABA<sub>A</sub> receptors in cultured murine hippocampal neurons. *J Neurosci.* 1994; 14:7747–7760. [PubMed: 7996209]
8. Adodra S, Hales TG. Potentiation, activation and blockade of GABA<sub>A</sub> receptors of clonal murine hypothalamic GT1-7 neurones by propofol. *Br J Pharmacol.* 1995; 115:953–960. [PubMed: 7582526]
9. Krasowski MD, Hong X, Hopfinger AJ, Harrison NL. 4D-QSAR analysis of a set of propofol analogues: mapping binding sites for an anesthetic phenol on the GABA<sub>A</sub> receptor. *J Med Chem.* 2002; 45:3210–3221. [PubMed: 12109905]
10. Chang CS, Olcese R, Olsen RW. A single M1 residue in the  $\beta_2$  subunit alters channel gating of GABA<sub>A</sub> receptor in anesthetic modulation and direct activation. *J Biol Chem.* 2003; 278:42821–42828. [PubMed: 12939268]
11. Bali M, Akabas MH. Defining the propofol binding site location on the GABA<sub>A</sub> receptor. *Molec Pharmacology.* 2004; 65:68–76.
12. Zecharia AY, et al. The involvement of hypothalamic sleep pathways in general anesthesia: testing the hypothesis using the GABA<sub>A</sub> receptor  $\beta_3N265M$  knock-in mouse. *J Neurosci.* 2009; 29:2177–2187. [PubMed: 19228970]
13. Jurd R, et al. General anesthetic actions *in vivo* strongly attenuated by a point mutation in the GABA<sub>A</sub> receptor  $\beta_3$  subunit. *FASEB J.* 2003; 17:250–252. [PubMed: 12475885]
14. Solt K, Forman SA. Correlating the clinical actions and molecular mechanisms of general anesthetics. *Curr Opin Anaesthesiol.* 2007; 20:300–306. [PubMed: 17620835]
15. Banghart M, Borges K, Isacoff E, Trauner D, Kramer RH. Light-activated ion channels for remote control of neuronal firing. *Nature Neurosci.* 2004; 7:1381–1386. [PubMed: 15558062]

16. Standaert RF, Park SB. Amino acids: design, synthesis and properties of new photoelastic amino acids. *J Org Chem.* 2006; 71:7952–7966. [PubMed: 17025282]
17. Volgraf M, et al. Allosteric control of an ionotropic glutamate receptor with an optical switch. *Nature Chem Biol.* 2006; 2:47–52. [PubMed: 16408092]
18. Fortin DL, et al. Photochemical control of endogenous ion channels and cellular excitability. *Nature Meth.* 2008; 5:331–338.
19. Janovjak H, Szobota S, Wyart C, Trauner D, Isacoff EY. A light-gated, potassium-selective glutamate receptor for the optical inhibition of neuronal firing. *Nature Neurosci.* 2010; 13:1027–1032. [PubMed: 20581843]
20. Beharry AA, Woolley GA. Azobenzene photoswitches for biomolecules. *Chem Soc Rev.* 2011; 40:4422–4437. [PubMed: 21483974]
21. Bali M, Akabas MH. The location of a closed channel gate in the GABA<sub>A</sub> receptor channel. *J Gen Physiol.* 2007; 129:145–159. [PubMed: 17227918]
22. Ueno S, Bracamontes J, Zorumski C, Weiss DS, Steinbach JH. Bicuculline and gabazine are allosteric inhibitors of channel opening of the GABA<sub>A</sub> receptor. *J Neurosci.* 1997; 17:625–634. [PubMed: 8987785]
23. Jones MV, Sahara Y, Dzubay JA, Westbrook GL. Defining affinity with the GABA<sub>A</sub> receptor. *J Neurosci.* 1998; 18:8590–8604. [PubMed: 9786967]
24. Amin J, Weiss DS. GABA<sub>A</sub> receptor needs two homologous domains of the  $\beta$ -subunit for activation by GABA but not by pentobarbital. *Nature.* 1993; 366:565–569. [PubMed: 7504783]
25. Muroi Y, Theusch CM, Czajkowski C, Jackson MB. Distinct structural changes in the GABA<sub>A</sub> receptor elicited by pentobarbital and GABA. *Biophys J.* 2009; 96:499–509. [PubMed: 19167300]
26. Wisden W, Korpi ER, Bahn S. The cerebellum: a model system for studying GABA<sub>A</sub> receptor diversity. *Neuropharmacol.* 1996; 35:1139–1160.
27. Fritschy J-M, Panzanelli P, Kralic JE, Vogt KE, Sassoè-Pognetto M. Differential dependence of axo-dendritic and axo-somatic GABAergic synapses on GABA<sub>A</sub> receptors containing the  $\alpha 1$  subunit in Purkinje cells. *J Neurosci.* 2006; 26:3245–3255. [PubMed: 16554475]
28. Wulff P, et al. From synapse to behavior: rapid modulation of defined neuronal types with engineered GABA<sub>A</sub> receptors. *Nature Neurosci.* 2007; 10:923–929. [PubMed: 17572671]
29. Meera P, Olsen RW, Otis TS, Wallner M. Etomidate, propofol and the neurosteroid THDOC increase the GABA efficacy of recombinant  $\alpha 4\beta 3\delta$  and  $\alpha 4\beta 3$  GABA<sub>A</sub> receptors expressed in HEK cells. *Neuropharmacology.* 2009; 56:155–160. [PubMed: 18778723]
30. Siegwart R, Jurd R, Rudolph U. Molecular determinants for the action of general anesthetics at recombinant  $\alpha 2\beta 3\gamma 2$   $\gamma$ -aminobutyric acid<sub>A</sub> receptors. *J Neurochem.* 2002; 80:140–148. [PubMed: 11796752]
31. Mihic SJ, Harris RA. Inhibition of  $\rho 1$  receptor GABAergic currents by alcohols and volatile anesthetics. *J Pharmacol Exp Ther.* 1996; 277:411–416. [PubMed: 8613949]
32. Kucken AM, et al. Identification of benzodiazepine binding site residues in the  $\gamma 2$  subunit of the  $\gamma$ -aminobutyric acid<sub>A</sub> receptor. *Molec Pharmacol.* 2000; 57:932–939. [PubMed: 10779376]
33. Kucken AM, Teissère JA, Seffinga-Clark J, Wagner DA, Czajkowski C. Structural requirements for imidazobenzodiazepine binding to GABA<sub>A</sub> receptors. *Molec Pharmacol.* 2003; 63:289–296. [PubMed: 12527800]
34. Ishida AT, Cohen BN. GABA-activated whole-cell currents in isolated retinal ganglion cells. *J Neurophysiol.* 1988; 60:381–396. [PubMed: 3171634]
35. Fischer KF, Lukasiewicz PD, Wong ROL. Age-dependent and cell class-specific modulation of retinal ganglion cell bursting activity by GABA. *J Neurosci.* 1998; 18:3767–3778. [PubMed: 9570807]
36. Wässle H, Koulen P, Brandstätter JH, Fletcher EL, Becker C-M. Glycine and GABA receptors in the mammalian retina. *Vision Res.* 1998; 38:1411–1430. [PubMed: 9667008]
37. Rotolo TC, Dacheux RF. Evidence for glycine, GABA<sub>A</sub> and GABA<sub>B</sub> receptors on rabbit OFF-alpha ganglion cells. *Visual Neurosci.* 2003; 20:285–296.
38. Häusser M, Clark BA. Tonic synaptic inhibition modulates neuronal output pattern and spatiotemporal synaptic integration. *Neuron.* 1997; 19:665–678. [PubMed: 9331356]

39. Smith SL, Otis TS. Persistent changes in spontaneous firing of Purkinje neurons triggered by the nitric oxide signaling cascade. *J Neurosci.* 2003; 23:367–372. [PubMed: 12533595]
40. Santhakumar V, Hancher HJ, Wallner M, Olsen RW, Otis TS. Contributions of the GABA<sub>A</sub> receptor  $\alpha 6$  subunit to phasic and tonic inhibition revealed by a naturally occurring polymorphism in the  $\alpha 6$  gene. *J Neurosci.* 2006; 26:3357–3364. [PubMed: 16554486]
41. Hestrin S, Nicoll RA, Perkel DJ, Sah P. Analysis of excitatory synaptic action in pyramidal cells using whole-cell recording from rat hippocampal slices. *J Physiol.* 1990; 422:203–225. [PubMed: 1972190]
42. Eisenman LN, et al. Anticonvulsant and anesthetic effects of a fluorescent neurosteroid analog activated by visible light. *Nature Neurosci.* 2007; 10:523–530. [PubMed: 17322875]
43. Trapani G, Altomare C, Sanna E, Biggio G, Liso G. Propofol in anesthesia. Mechanism of action, structure-activity relationships, and drug delivery. *Curr Med Chem.* 2000; 7:249–271. [PubMed: 10637364]
44. Baulac S, et al. First genetic evidence of GABA<sub>A</sub> receptor dysfunction in epilepsy: a mutation in the  $\gamma 2$ -subunit gene. *Nature Genetics.* 2001; 28:46–48. [PubMed: 11326274]
45. Palma E, et al. Abnormal GABA<sub>A</sub> receptors from the human epileptic hippocampal subiculum microtransplanted to *Xenopus* oocytes. *Proc Natl Acad Sci USA.* 2005; 102:2514–2518. [PubMed: 15695331]
46. Goodkin HP, Joshi S, Mtchedlishvili Z, Brar J, Kapur J. Subunit-specific trafficking of GABA<sub>A</sub> receptors during status epilepticus. *J Neurosci.* 2008; 28:2527–2538. [PubMed: 18322097]
47. Macdonald RL, Kang J-Q, Gallagher MJ. Mutations in GABA<sub>A</sub> receptor subunits associated with genetic epilepsies. *J Physiol.* 2010; 588:1861–1869. [PubMed: 20308251]
48. Power KN, Flaatten H, Gilhus NE, Engelsen BA. Propofol treatment in adult refractory status epilepticus. Mortality risk and outcome. *Epilepsy Res.* 2011; 94:53–60. [PubMed: 21300522]
49. Iyer VN, Hoel R, Rabinstein AA. Propofol infusion syndrome in patients with refractory status epilepticus: an 11-year clinical experience. *Crit Care Med.* 2009; 37:3024–3030. [PubMed: 19661801]
50. Rossetti AO, Lowenstein DH. Management of refractory status epilepticus in adults: still more questions than answers. *Lancet Neurol.* 2011; 10:922–930. [PubMed: 21939901]
51. Yizhar O, Fenno LE, Davidson TJ, Mogri M, Deisseroth K. Optogenetics in neural systems. *Neuron.* 2011; 71:9–34. [PubMed: 21745635]
52. Qian H, Dowling JE. GABA<sub>A</sub> and GABA<sub>C</sub> receptors on hybrid bass retinal bipolar cells. *J Neurophysiol.* 1995; 74:1920–1928. [PubMed: 8592185]
53. Lukasiewicz PD, Shields CR. Different combinations of GABA<sub>A</sub> and GABA<sub>C</sub> receptors confer distinct temporal properties to retinal synaptic responses. *J Neurophysiol.* 1998; 79:3157–3167. [PubMed: 9636116]
54. Palmer MJ. Functional segregation of synaptic GABA<sub>A</sub> and GABA<sub>C</sub> receptors in goldfish bipolar cell terminals. *J Physiol.* 2006; 577:45–53. [PubMed: 17008372]
55. Yue L, et al. Potentiating action of propofol at GABA<sub>A</sub> receptors of retinal bipolar cells. *Invest Ophthalmol Vis Sci.* 2011; 52:2497–2509. [PubMed: 21071744]
56. Xie A, et al. Propofol potentiates GABA-elicited responses of bipolar and ganglion cells in rat retina. *Invest Ophthalmol Vis Sci.* 2010; 51 ARVO E-abstract 1865.
57. Sadvoski O, Beharry AA, Zhang F, Woolley GA. Spectral tuning of azobenzene photoswitches for biological applications. *Angew Chem Int Ed.* 2009; 48:1484–1486.
58. Adamian L, et al. Structural model of  $\rho 1$  GABA<sub>C</sub> receptor based on evolutionary analysis: testing of predicted protein-protein interactions involved in receptor assembly and function. *Protein Sci.* 2009; 18:2371–2383. [PubMed: 19768800]
59. Ramsey DJ, Ripps H, Qian H. Streptozotocin-induced diabetes modulates GABA receptor activity of rat retinal neurons. *Exper Eye Res.* 2007; 85:413–422. [PubMed: 17662714]
60. Gorostiza P, Isacoff EY. Optical switches for remote and noninvasive control of cell signaling. *Science.* 2008; 322:395–399. [PubMed: 18927384]

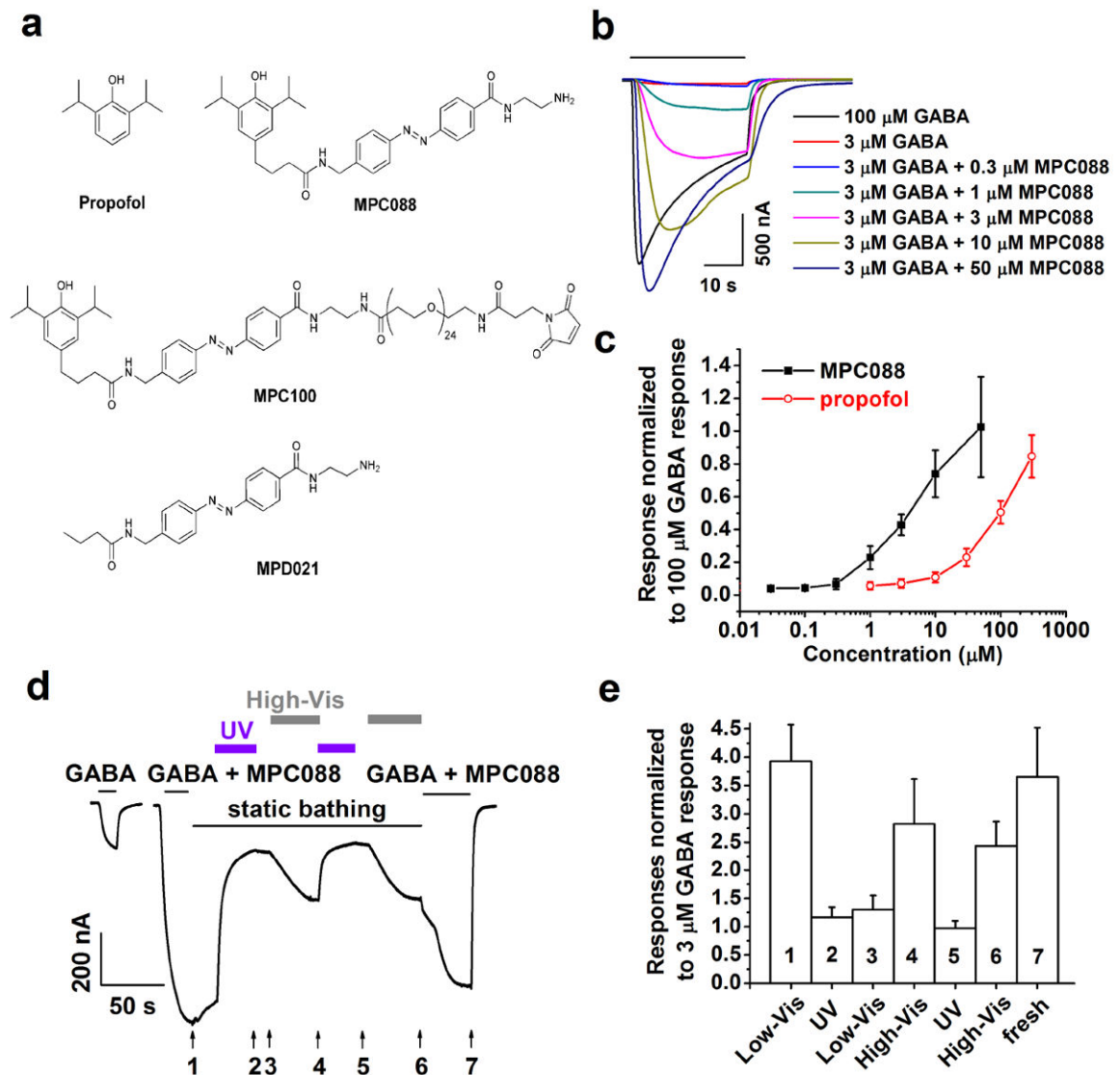


**Figure 1. Effect of MPC088 on the 3  $\mu$ M GABA response of  $\alpha_1\beta_2\gamma_2$  GABA<sub>A</sub>R-expressing oocytes**  
**a:** Chemical structures. **b:** Responses of a single oocyte to co-applied 3  $\mu$ M GABA and varying concentration of *trans*-dominant MPC088. Horizontal bar indicates the period of superfusion with GABA- and MPC088-supplemented Ringer solution. **c:** Aggregate concentration-response data (mean  $\pm$  SD) describing responses elicited by co-applied 3  $\mu$ M GABA and *trans*-dominant MPC088 or propofol. Response amplitudes obtained from each oocyte normalized to that elicited by 100  $\mu$ M GABA alone, a near-saturating condition that is essentially insensitive to propofol potentiation. MPC088 and propofol results, each obtained from 7 oocytes. **d:** Light-dependent alteration of the 3  $\mu$ M GABA response by co-applied, initially *trans*-dominant, 1  $\mu$ M MPC088. *Black bars:* periods of superfusion with co-applied 3  $\mu$ M GABA and 1  $\mu$ M MPC088. *Purple and gray bars:* period of presentation of UV light and high-intensity visible light (High-Vis), respectively. **e:** Results obtained in the experiment of **d** and 3 others of similar design (mean  $\pm$  SD). Membrane current amplitudes, normalized to the peak amplitude of the 3  $\mu$ M GABA response, determined under 7



sequential conditions: (1) in low-intensity visible light (Low-Vis), at the conclusion of superfusion with (3  $\mu$ M GABA + 1  $\mu$ M MPC088); (2) at the conclusion of UV illumination; (3) in low-intensity visible light; (4) at the conclusion of high-intensity visible illumination; (5) at the conclusion of a second UV illumination; (6) at the conclusion of a second high-intensity visible illumination; and (7) at the conclusion of resumed superfusion with fresh 3  $\mu$ M GABA + 1  $\mu$ M *trans*-dominant MPC088. These amplitude determination conditions are denoted by numbers beneath the waveform in **d**. Repeated-measures ANOVA conducted on the aggregate data yielded  $F(6,18) = 41.975$ ,  $p < 0.001$ . Post-hoc paired-sample *t*-tests corrected for multiple comparisons indicated significant differences produced by the initial UV, the initial High-Vis, the second UV, and the second High-Vis illuminations ( $p = 0.009$  for amplitude group 2 *vs.* group 1, for 4 *vs.* 3, for 5 *vs.* 4, and for 6 *vs.* 5, respectively); amplitude groups 7 and 1 did not differ significantly ( $p = 0.075$ ).

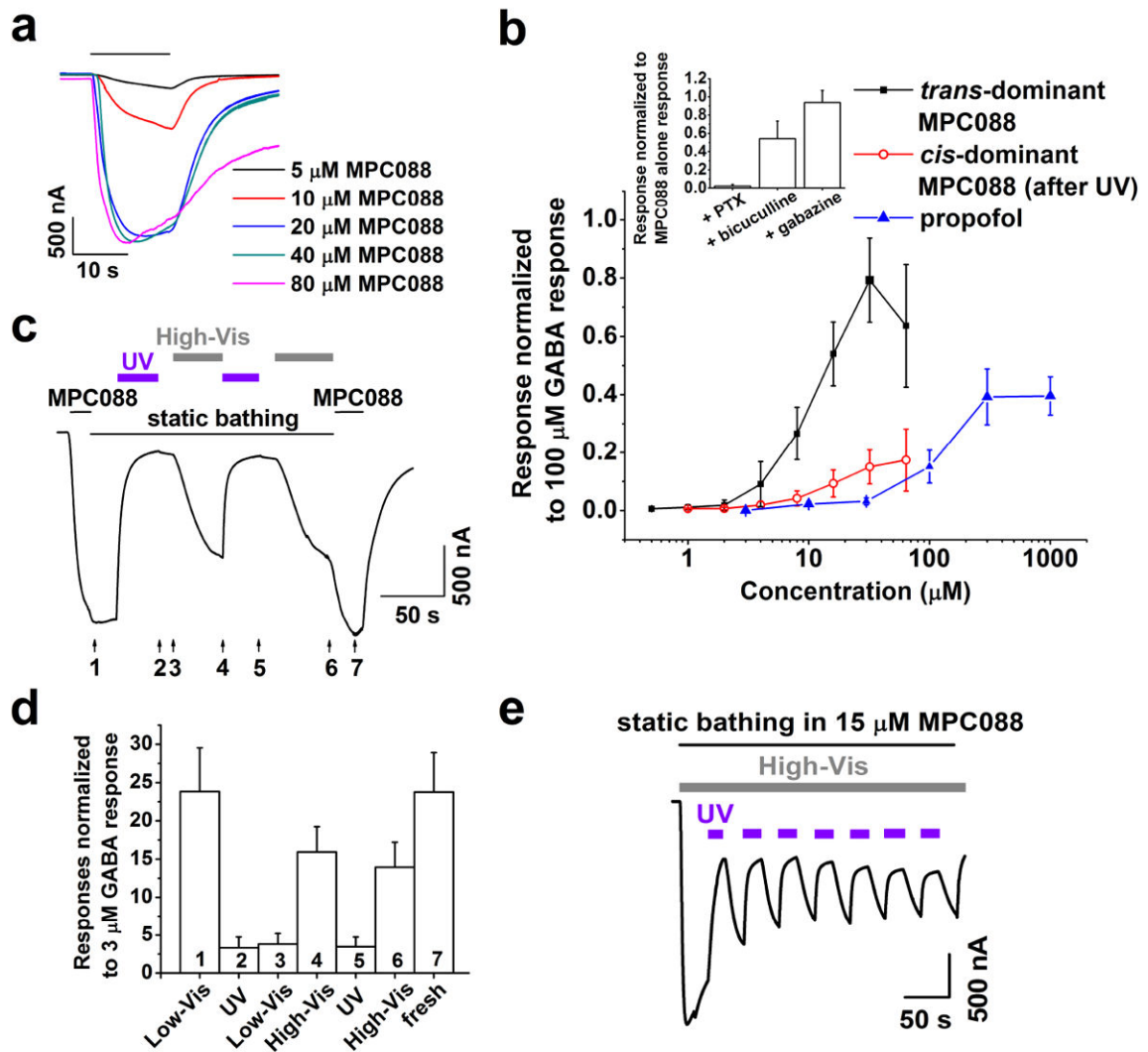


**Figure 2. MPC088 agonist activity in oocytes expressing  $\alpha_1\beta_2\gamma_2$  GABA<sub>A</sub>Rs**

**a:** Representative responses to MPC088 obtained in a single experiment. **b:** Concentration-response functions (mean  $\pm$  SD) for *trans*- and *cis*-dominant MPC088 ( $n = 6$ ) and propofol ( $n = 6$ ). In each of the MPC088 experiments, the *cis*-dominant form was generated by UV light during static bathing. Amplitudes normalized to the 100  $\mu\text{M}$  GABA response. *Inset:* Sensitivity (mean  $\pm$  SD) of the MPC088 (15  $\mu\text{M}$ ) response to 100  $\mu\text{M}$  PTX ( $n = 4$ ), 100  $\mu\text{M}$  bicuculline ( $n = 4$ ) and 30  $\mu\text{M}$  gabazine ( $n = 4$ ). **c:** Photo-regulation of the response to 15  $\mu\text{M}$  MPC088. **d:** Normalized current amplitudes (mean  $\pm$  SD) determined in the experiment of **c** and in 3 others of similar design. Amplitudes in each experiment normalized to that elicited by 3  $\mu\text{M}$  GABA. Numbers beneath the waveform in **c** denote amplitude determination conditions for the experiment shown in **c**. Repeated-measures ANOVA conducted on the aggregate data yielded  $F(6,18) = 68.988$ ,  $p < 0.001$ . Post-hoc paired-sample *t*-tests corrected for multiple comparisons indicated significant differences produced by the initial UV, the initial High-Vis, the second UV, and the second High-Vis illuminations ( $p = 0.010$  for amplitude group 2 vs. group 1, for 4 vs. 3, for 5 vs. 4, and for 6

vs. 5, respectively); amplitude groups 7 and 1 did not differ significantly ( $p = 0.96$ ). **e:** Representative waveform obtained with repeated presentation of UV light during continuous High-Vis illumination (static bathing in MPC088-supplemented Ringer).

Author Manuscript

Author Manuscript

Author Manuscript

Author Manuscript

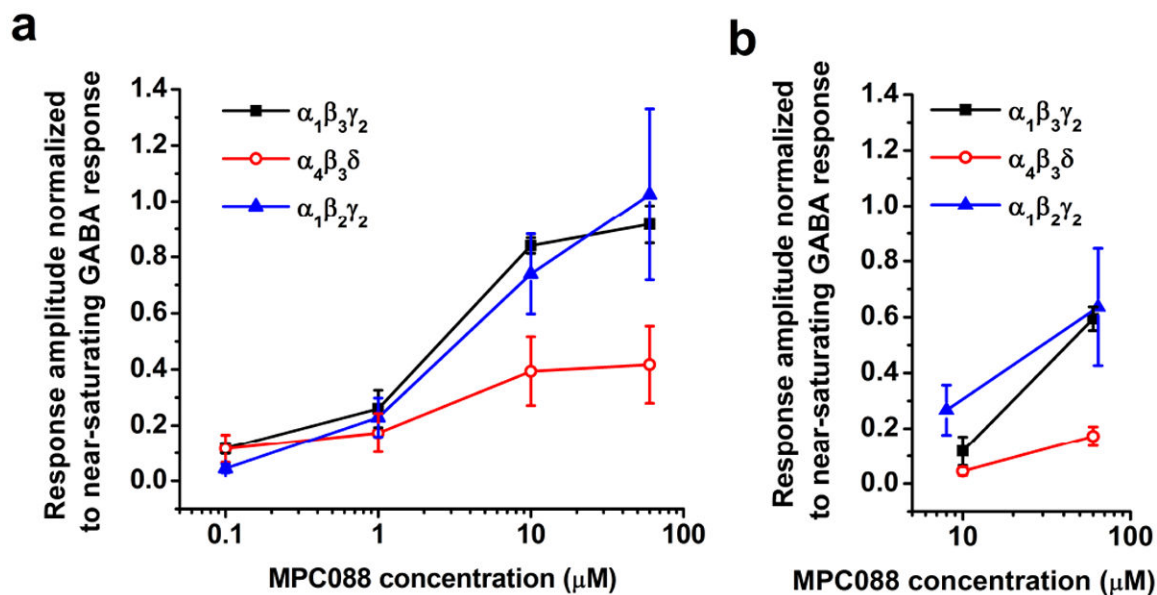


**Figure 3. Effect of MPC088 on  $\alpha_1\beta_3\gamma_2$  and  $\alpha_4\beta_3\delta$  GABA<sub>A</sub>R-expressing oocytes**

Data in each group obtained from 4 oocytes. **a:** Aggregate concentration-response data (mean  $\pm$  SD) obtained from  $\alpha_1\beta_3\gamma_2$  (black) and  $\alpha_4\beta_3\delta$  (red) receptors with co-applied GABA at similar  $\sim\text{EC}_3$  dose (i.e., 3  $\mu\text{M}$  for the former and 0.05  $\mu\text{M}$  for the latter receptor type) and varying concentrations of *trans*-dominant MPC088. Response amplitudes obtained from each oocyte normalized to its saturating GABA response (i.e., responses obtained with 1,000  $\mu\text{M}$  GABA for  $\alpha_1\beta_3\gamma_2$  and 100  $\mu\text{M}$  GABA for  $\alpha_4\beta_3\delta$  GABA<sub>A</sub>Rs). **b:** Aggregate concentration-response data (mean  $\pm$  SD) obtained from  $\alpha_1\beta_3\gamma_2$  (black) and  $\alpha_4\beta_3\delta$  (red) receptors with *trans*-dominant MPC088 alone. Data similarly normalized to the saturating GABA response obtained from each oocyte. Results for  $\alpha_1\beta_2\gamma_2$  GABA<sub>A</sub>Rs in **a** and **b** (blue) reproduced from those of Figures 1c and 2b, respectively.

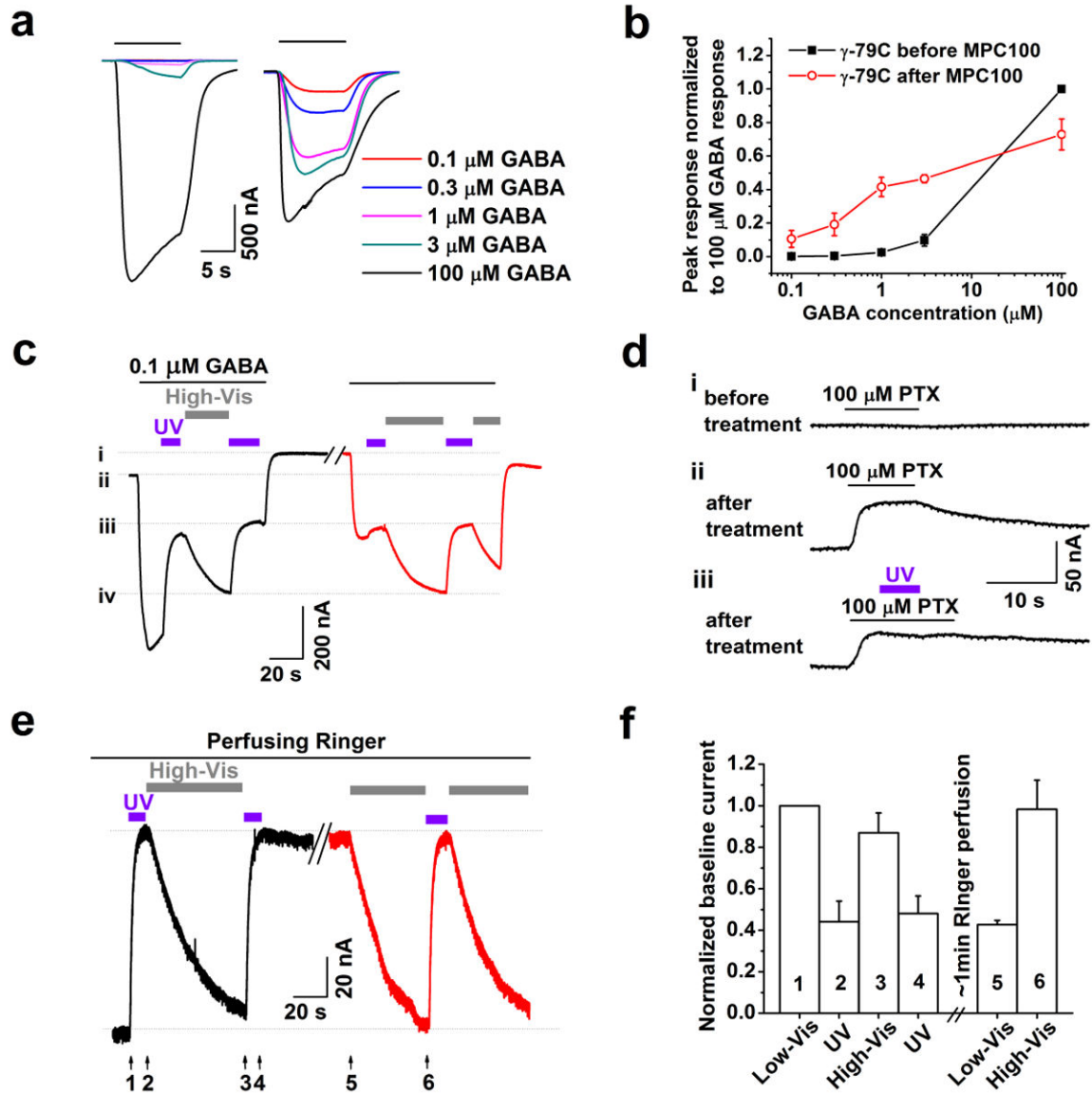


**Figure 4. Persistent potentiation and activation by MPC100 in  $\gamma$ -79C-expressing oocytes**  
**a:** GABA responses of a single oocyte before (*left*) and after (*right*) MPC100 treatment (100  $\mu\text{M}$ ). Right-hand waveforms recorded after  $\sim 7$ -min incubation with MPC100 and subsequent Ringer perfusion. **b:** GABA response functions showing aggregate data (mean  $\pm$  SD; 5 oocytes) obtained before MPC100 treatment, and after treatment with 100  $\mu\text{M}$  MPC100 and subsequent washout ( $\sim 5$  min). Amplitudes normalized to that elicited by 100  $\mu\text{M}$  GABA before MPC100 treatment. **c:** Light-dependence of persistent potentiation. *Black trace:* response to UV and visible light in the presence of 0.1  $\mu\text{M}$  GABA, following treatment with 100  $\mu\text{M}$  *trans*-dominant MPC100. Dotted lines i and ii highlight the difference in baseline current before (ii) vs. after (i) UV illumination). *Red trace:* later phase of the same experiment (responses obtained after a further  $\sim 1$  min Ringer perfusion). **d:** Baseline currents obtained in a single experiment. Trace (i): nominal response to PTX (100  $\mu\text{M}$ ). Traces ii-iii: PTX responses obtained after treatment with 100  $\mu\text{M}$  MPC100, in the absence

(ii) and presence (iii) of UV illumination. **e**: Responses to UV and visible light following exposure to *trans*-dominant MPC100 and washout (~5 min) of free MPC100. Data obtained from a single oocyte. A period of Ringer perfusion (~1 min) separated the initial (*black trace*) and later (*red trace*) phases of the experiment. **f**: Aggregate results (mean  $\pm$  SD) from experiment **e** and 3 others, each involving amplitude determinations under 6 sequential experimental conditions. Data normalized to the persisting shift in baseline produced by MPC100 treatment. Periods of treatment in each experiment were similar to those illustrated in **e**. Numbers beneath the waveforms in **e** denote amplitude determination conditions for the experiment shown in **e**. Repeated-measures ANOVA conducted on the aggregate data yielded  $F(6,18) = 65.290$ ,  $p < 0.001$ . Post-hoc paired-sample *t*-tests corrected for multiple comparisons indicated significant differences produced by the initial UV, the initial High-Vis, the second UV, and the second High-Vis illuminations ( $p = 0.007$  for amplitude group 2 vs. group 1, for 3 vs. 2, for 4 vs. 3, and for 6 vs. 5, respectively).

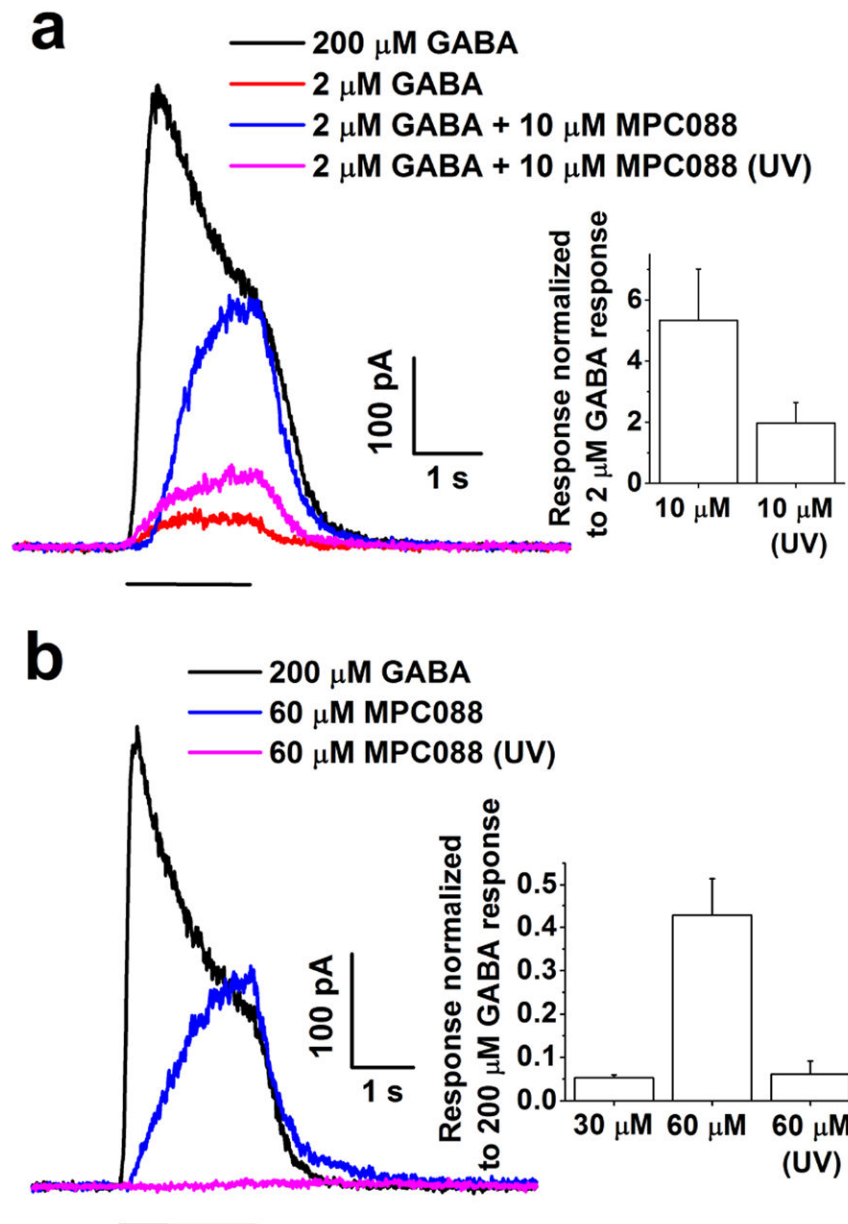


**Figure 5. Action of MPC088 on retinal ganglion cells**

**a:** Potentiation data obtained with *trans*- and *cis*-dominant MPC088; the *cis*-dominant preparation was obtained by pre-treating *trans*-dominant MPC088 with UV light for 5 min. Representative responses obtained from a single cell treated with 200  $\mu\text{M}$  GABA (*black*), 2  $\mu\text{M}$  GABA (*red*), 2  $\mu\text{M}$  GABA co-applied with 10  $\mu\text{M}$  of *trans*-dominant (*blue*) or *cis*-dominant (*magenta*) MPC088. *Inset:* Aggregate data (mean  $\pm$  SD) for potentiation factor determined with *trans*- and *cis*-dominant MPC088 (*left* and *right* bars, respectively) ( $n=6$ ,  $p = 0.003$ ). **b:** Direct activation data obtained with *trans*- and *cis*-dominant MPC088. Representative responses obtained from a cell treated with 200  $\mu\text{M}$  GABA (*black*), 60  $\mu\text{M}$  of *trans*-dominant (*blue*) and 60  $\mu\text{M}$  of *cis*-dominant (*magenta*) MPC088. *Inset:* Aggregate data (mean  $\pm$  SD) for direct activation by MPC088. *Left*, *middle* and *right* bars show results

obtained, respectively, with 30  $\mu\text{M}$  *trans*-dominant (n=3), 60  $\mu\text{M}$  *trans*-dominant (n=7), and 60  $\mu\text{M}$  *cis*-dominant MPC088 (n=4).

Author Manuscript

Author Manuscript

Author Manuscript

Author Manuscript



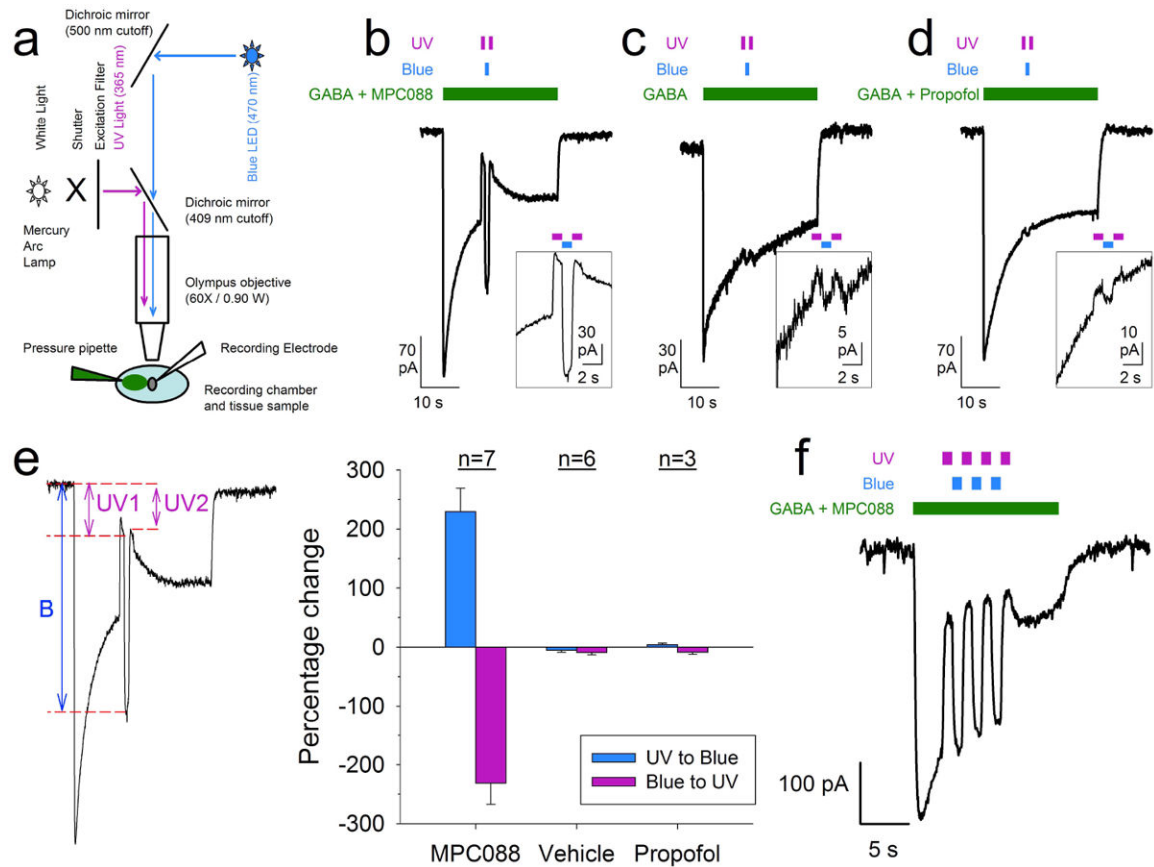


**Figure 6. Effect of MPC088 photoactivation on GABA-evoked currents in cerebellar PNs**  
**a:** Optical configuration. **b:** Representative trace from a whole-cell voltage-clamp recording from a PN. The cell was held at -70 mV, and 10  $\mu$ M GABA + 30  $\mu$ M MPC088 were applied via pressure pipette for 30 s. The cell was flashed with UV light (1 s, shuttered from a mercury arc lamp), then blue light (1 s, from a 470 nm LED), and then again with UV light (1 s). Insets expand the segments of the trace recorded when the light pulses were delivered. **c:** Trace from the same cell as in **b**, but with exposure to 10  $\mu$ M GABA alone. **d:** Trace from the same cell as in **b-c**, but with exposure to 10  $\mu$ M GABA + 300  $\mu$ M propofol. **e:** Summary of results described in **b-d**. The left-hand trace shows the method used to obtain the numerical data shown at the right. The magnitude of the UV-to-blue transition was calculated as  $(B-UV1)/UV1$ ; that of the blue-to-UV transition was calculated as  $(UV2-B)/UV2$ . Here, UV1, B and UV2 are, respectively, the magnitude of the current evoked by the first UV flash, the blue flash and the second UV flash, as referenced to the pre-GABA current level. The number above each condition indicates the number of cells from which data were obtained. For the negative control experiments (i.e., those involving exposure to vehicle or propofol alone) in which no light-evoked current was detectable, current was measured for identical epochs at the terminations of the light pulses. Error bars represent the SEM. For both the blue-to-UV and the UV-to-blue transitions, the Kruskal-Wallis ANOVA on Ranks yielded  $p < 0.005$  ( $H > 11$ ,  $df = 2$ ). Post-hoc statistical tests showed that results obtained with MPC088 treatment differed significantly from those obtained under either negative control condition (Mann-Whitney Rank-Sum Test: MPC088 vs. vehicle (blue-to-

UV and UV-to-blue),  $p = 0.002$ ; MPC088 vs. propofol (blue-to-UV and UV-to-blue),  $p = 0.014$ ;  $p$  values adjusted for multiple comparisons). **f**: Representative trace from a cell exposed to multiple UV/blue light flashes during application of GABA and MPC088.

Author Manuscript

Author Manuscript

Author Manuscript

Author Manuscript

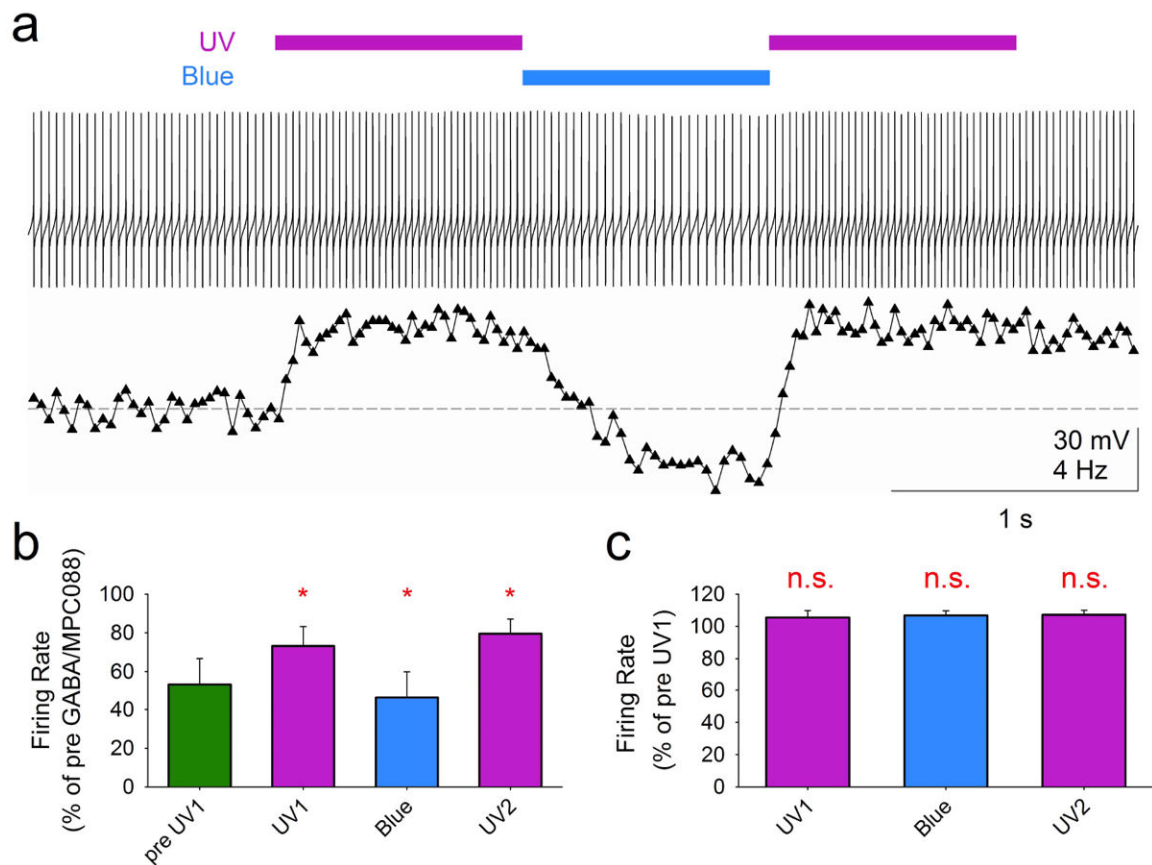


**Figure 7. Effect of MPC088 photoactivation on action potential firing frequency in PNs**  
**a:** Representative data obtained by whole-cell current-clamp recording from a PN which was injected with 468 pA to elicit a high-frequency train of action potentials. During this current step, 10  $\mu$ M GABA + 30  $\mu$ M *trans*-dominant MPC088 were applied via pressure pipette for 10 s. The cell was then exposed for 1-s durations to UV light (UV1), then blue light, and then again with UV (UV2). The entire illustrated voltage vs. time trace occurs during application of GABA/MPC088. Below this trace is plotted the instantaneous firing frequency vs. time; the dashed line reflects the average firing frequency during the 1-s epoch that preceded the first UV exposure. **b:** Summary of results from experiments of the type shown in **a**. Average spike frequencies were obtained for each cell in each of five 1-s epochs, then normalized to the pre-GABA/MPC088 firing frequency ( $n = 8$  cells from 4 animals). Error bars here and in **c** represent the SEM. Repeated-measures ANOVA on the aggregate data yielded  $F(3,21) = 10.213$ ,  $p < 0.001$ . Red asterisks above the purple and blue bars indicate significance of the average frequency in that epoch vs. the preceding epoch (e.g., the asterisk above the UV1 bar refers to significance of the average firing rate in the UV1 epoch vs. the GABA/MPC088 pre-UV epoch). Significance was determined from post-hoc paired-sample *t*-tests corrected for multiple comparisons, which yielded  $p < 0.02$ . **c:** Summary of results from experiments similar to that described in **a**, but in which the cell was exposed only to the UV/Blue/UV flash sequence (i.e., no GABA/MPC088 applied). Data normalized to the average firing frequency during the 1-s period preceding the first UV flash ( $n = 7$  cells from 3 animals). Repeated-measures ANOVA on the aggregate data

yielded  $F(3,18) = 3.057$ ,  $p > 0.05$ . Three post-hoc statistical tests were then performed as described in **b**; none of these yielded significance at the uncorrected 0.05 level.

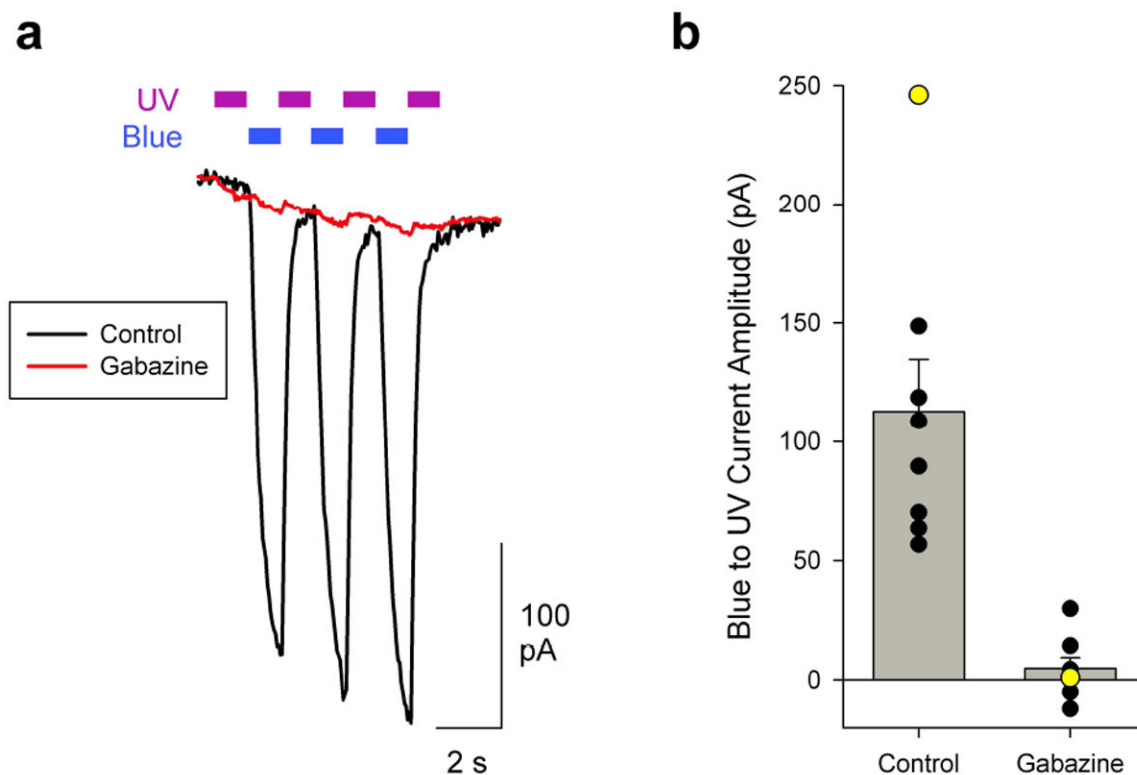


**Figure 8. Lack of agonist activity of MPC088 on PNs**

**a:** Averages of 10 recordings from a PN exposed to multiple Blue/UV light flashes, in the presence of *cis*-dominant MPC088 (30  $\mu$ M) in the external solution, before (*black*) and after (*red*) the addition of gabazine (30  $\mu$ M). There was no exogenous GABA present in the tissue. **b:** Summary of results from 8 experiments (8 PNs) including that described in **a**. The data indicate the magnitude of an outward current. The temporal sequence of illumination differed among the experiments (e.g., only the cell in **a** received multiple blue/UV exposures), but the data plotted are the amplitudes from the blue to UV transition (in the case of the cell in **a**, this is the blue/UV transition from the first of the three exposures). Yellow-filled data points indicate results from the experiment in **a**. Each data point is the average obtained from 4-10 consecutive recordings. The light-evoked membrane current was significantly reduced by gabazine (Wilcoxon Signed Rank Test,  $p=0.008$ ). Error bars represent the SEM.